



## DESIGNING OF COPPER OXIDE-LOADED CASEIN NANOPARTICLES AND THEIR RELEASE POTENTIAL

**Preeti Burvey<sup>1</sup>**

Department of Chemistry, Medi-caps University, Indore-453331, (M.P.) India

Email: pburvey@hotmail.com

**Preeti Jain<sup>2\*</sup>**

Medi-caps University Indore M.P.

Email: preetijain278gmail.com

**Anamika Singh<sup>3</sup>**

Mata Jija Bai girl's college Indore

Email: singhanamika16488@gmail.com

**\*Corresponding Author:** Preeti Jain\*Professor, Department of Chemistry Medi-caps University Indore M.P. Email: preetijain278gmail.com

**ABSTRACT**

The design of controlled delivery systems for a variety of applications connected to pharmaceuticals, food-related bioactive substances, agro-chemicals, etc., benefits from the versatility in polymer processing. Natural polymers often have a more complex chemical arrangement than synthetic polymers since they are produced by an organism or plant. The emulsion cross-linking approach was used to create casein nanoparticles. Copper oxide deposition inside the casein matrix was done in-situ to create copper oxide-loaded casein nanoparticles. With the use of XRD, FTIR, XPS analysis, and Raman spectroscopy, the interactions of nanoparticles of casein with copper oxide were investigated. The created nanoparticles have shown capacity as tiny vehicles that can transport various substances to specific sites. As we look ahead, these nanoparticles could play a crucial role in delivering loaded components to targeted areas.

Keywords: Nanotechnology, Copper oxide-loaded casein nanoparticles, Crop productivity, Micronutrients, soil quality

**1.0 Introduction**

Nanotechnology encompasses all technologies that operate at the Nano scale and have real-world applications. The process referred to involves the manipulation and organization of substances on an atomic and molecular scale, typically within a size range of 1 to 100 nanometres[1]. The manipulation and design of materials at the Nano scale are the primary focus of nanotechnology, where physical and chemical properties can differ substantially from their bulk counterparts[2]. As a material decreases in size, its properties initially remain unchanged; however, significant changes may occur over time. This fact has made nanotechnology an exciting and rapidly growing interdisciplinary field with countless potential real-world applications, including agriculture, health, and pharmaceuticals. Recently, there has been an increasing interest in the potential agricultural applications of nanotechnology[3].

Black soils are made up of fine clayey materials and are well-known for their excellent moisture retention capacity and high nutrient content, including calcium carbonate, magnesium, potash, and lime[4]. Soil fertility is determined by essential soil elements, including macronutrients (like N, K, and P) and micronutrients (such as Fe, B, Mo, Cl, Mn, Zn, and Cu). Topsoil is a crucial resource for plants as it contains humus, which supports biological activity, enhances soil fertility, and regulates air and water content [5].

Ensuring soil fertility and providing adequate plant nutrition is crucial for the sustenance and well-being of all living organisms. As the global population continues to grow, there is increasing pressure on soil to provide essential nutrients, and the need to enhance food and fibre production becomes more significant. In response to the limitations of micronutrients, the application of micronutrient fertilizers has been

developed in recent decades[6]. However, delivering small amounts evenly over the target area remains a major challenge in the fertilization process, often increasing the cost of the application process itself rather than the product[7]. The most common method of delivering micronutrients involves mixing them with macronutrient fertilizers, which are used simultaneously. While this approach is generally effective, it is not without limitations. A viable alternative involves synthesizing micronutrients such as iron, copper, zinc and others in Nano scale form to produce controlled nano-fertilizers that can overcome the limitations of traditional fertilizers[8]. Copper oxide combined with biopolymers such as silk, casein, gelatine, and CMC form polymeric nano-composites that have been shown to have agricultural applications. These Nano-composites are particularly useful in the development of controlled-release (CR) formulations for crop production and protection[9].

Polymeric Nano-composites have a significant role in the development of controlled release formulations for crop production and crop protection, as stated in numerous studies. Slow-release fertilizers, which have low solubility, gradually provide nutrients for an extended period, improving fertilizer nutrient uptake efficiency while minimizing leaching losses. To address the challenges of slow agrochemical delivery, Nano-composites were designed. Due to their high durability and extended shelf life, they are ideal for use in agricultural field conditions[10].

## **2.0 EXPERIMENTATION**

### **2.1 MATERIALS& METHODOLOGY**

#### **Preparation of Copper-oxide Loaded Casein Nano-particles**

The process of preparing casein nanoparticles loaded with copper oxide is a simple two-step approach. The 1st step involves creating the casein nanoparticles, while the 2nd step involves impregnating copper oxide within the matrix of the casein nanoparticles[11].

#### **Formation of Casein Nano-particles**

To produce casein nano-particles, a micro-emulsion technique was employed, which was outlined in investigation[12]. A solution of casein was dissolved in a 1% basic solution of NaOH to create an "aqueous phase," while toluene was utilized as the "oil phase." Then casein and toluene solutions were combined and vigorously mixed using a magnetic stirrer for duration of 30 minutes. Then, 2 ml glutaraldehyde added to the emulsion as a cross-linker, followed by constant stirring at room temperature (30°C) for 30 minutes. Finally, HCl was added to solidify the particles. The particles were washed 3.4 times with acetone and stored in air-tight container after preparation[13].

#### **Impregnation of Fe into the Casein nanoparticles**

After drying, the nanoparticles were added to a water-based mixture containing Fe<sup>2+</sup> chloride salts. They were left to absorb the mixture for 24 hours, which resulted in the entrapment of Fe<sup>2+</sup> and Fe<sup>3+</sup> ions within the biopolymer matrices, specifically casein. To manage the reaction speed, which is closely tied to how fast the iron species oxidizes, a dry N<sub>2</sub> stream was passed over them for at least 15 minutes before immersing them in the salt solution. Additionally, nitrogen gas was bubbled through the solution to safeguard against excessive oxidation of the magnetite and to decrease the size of the particles. Another indication of iron oxide development can be seen in the vibrant orange to deep brown colour change of casein nanoparticles. After being cleaned, the nanoparticles were allowed to air dry at room temperature before being placed in an airtight container for storage. To calculate the loading % of impregnated iron oxide, the following equation may be used[14].

### 3.0 Characterization Technique

Various techniques are employed to discuss characterization techniques; Spectroscopy is used to investigate the correlation between radiation and matter in terms of electromagnetic wave wavelength, which facilitates the recognition of the chemical composition, crystal structure, and photoelectric properties of materials. There are numerous techniques available for this purpose, including Raman spectroscopy, Powder X-ray diffraction pattern analysis (PXRD), X-ray photoelectron spectroscopy (XPS), and Fourier transform infrared spectroscopy (FTIR). Furthermore, microscopy is an approach that is employed to examine the surface and sub-surface structure of polymer matrix. The stability of nanoparticles can be determined using zeta potential, with the magnitude of the zeta potential providing insight into particle stability. Since casein is a polymer, optical microscopy TEM is not needed and only SEM suffices[15].

## 4.0 Result and discussion

### 4.0.1 PXRD

The researchers employed the powder X-ray diffraction method to identify the crystalline nature of the casein nanoparticles that contained copper oxide.

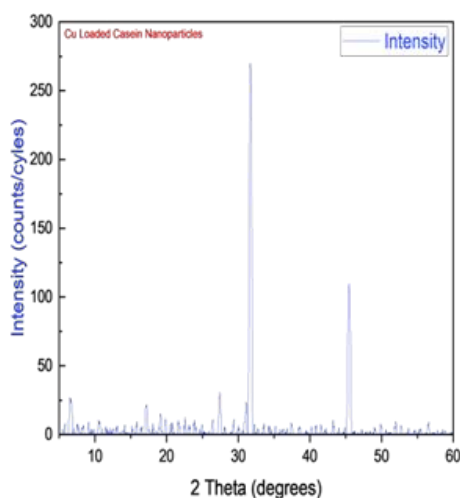


Figure 1 PXRD of Cu loaded nanoparticles

We used X-ray diffraction to analyse the crystalline arrangement of the nanoparticles. The data was collected by measuring  $2\theta$  values from  $10^\circ$  to  $80^\circ$ , The measurements were taken using a step size of 0.02, with each step lasting 2 seconds to determine the degree of crystallinity of both the casein and copper oxide loaded casein nanoparticles, an equation was used. This helped the researchers to distinguish between the crystalline and amorphous properties of the nanoparticles[16].

$$X_c(\%) = \frac{A_c}{A_a + A_c} \times 100$$

In order to assess the proportions of crystalline and non-crystalline components in the sample, we measured the areas of  $A_c$  and  $A_a$ . Additionally, Scherer's formula was utilized to evaluate the size of the copper oxide particles.

$$d = k \frac{\lambda}{\beta \cos \theta}$$

Scherer's formula was used to estimate the regular size of copper oxide particles. The formula involves variables such as the grain size 'd', the shape factor 'k' (0.9), the diffraction angle ' $\beta$ ', and the wavelength of diffraction ' $\lambda$ ' (1.54 Å).[17].

The Cu loaded casein nanoparticles were confirmed to have a percent crystallinity of 56%. This high percentage suggests that the copper oxide has been successfully embedded within the casein nanoparticle matrix; given that casein itself is typically amorphous in nature. Moreover, XRD measurements were employed to determine the average grain size of the prepared nanoparticles. The copper-infused casein nanoparticles were observed to have an estimated size of around 48.3 nm. To validate the effective incorporation of copper oxide into the casein nanoparticles, the peak position and corresponding "d" values were compared with the reference JCPDS data file no. 83-1665. This comparison confirmed the successful deposition of copper oxide in the nanoparticles. This comparison provided further evidence of the successful incorporation of copper oxide into the casein nanoparticles[18].

#### 4.0.2 FTIR

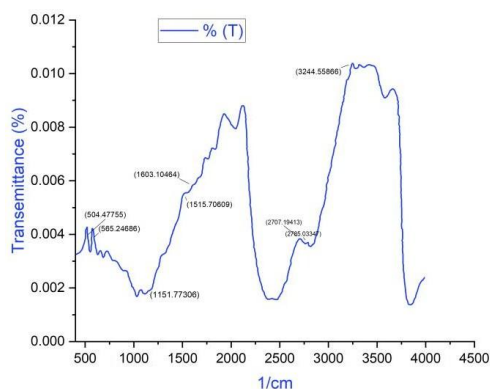


**Figure 2** FTIR of Cu O loaded casein nanoparticles

The FTIR spectra displayed characteristic bands at 1151 (1/cm), 565 (1/cm), 504 1/cm 1515 (1/cm), 1603 (1/cm), and 3244 (1/cm) for the nanoparticles annealed at 400°C, as depicted in Figure 2. Examining the nature of copper oxide nanoparticles is crucial to ensure their purity, and FTIR spectra can provide valuable information in this regard. The presence of peaks at 2707 (1/cm) and 2785 (1/cm) can be attributed to the asymmetric and symmetric stretching vibrations of C-H bonds, respectively [19]. The vibrations observed at 504 (1/cm) correspond to Cu<sub>2</sub>O, while the vibrations at 565 (1/cm) are characteristic of Cu O. The bending and stretching the bond at 1151 (1/cm) comes from C=O. The H–O–H bending at 1603 (1/cm) and O–H stretching at 3244 (1/cm) were also observed[20].

#### 4.0.3 SEM Technique

Figures (3A and 3 B) present SEM images of Cu-loaded casein nanoparticles.

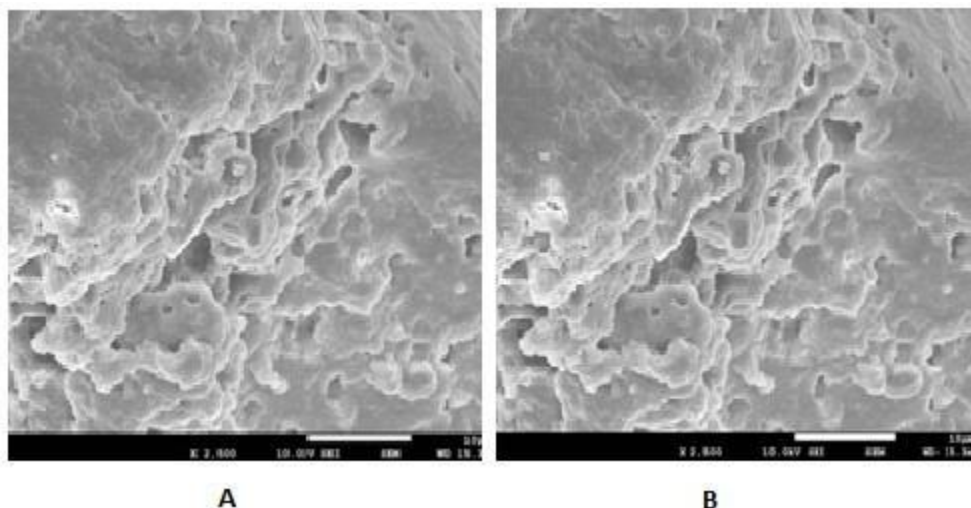


Figure 3(A and B) - SEM of Cu loaded casein

The pictures clearly display the uneven, rough appearance of casein nanoparticles and the position of Cu within the casein structure. When casein coating is applied to copper oxide, it results in the formation of larger particles. This is because the coating layers are created on the surfaces of the oxide, contributing to the particle enlargement. The copper oxides are attached to both the external and internal surfaces of the polymer matrix, and the structural soundness and morphology are influenced by the loading of Cu inside the matrix[21]. The biopolymer networks might be utilized as nano-reactors to build or assemble copper oxide. The formation of copper oxide clusters is influenced by multiple factors, including the coordination bond between copper and oxygen on the surface, the steric effects, and the compartmentalization within the casein matrix structures. These elements restrict the growth of copper oxide in the network, resulting in the formation of clusters. Compared to casein nanoparticles, which have an uneven size distribution, the degree of clustering in Cu-loaded nanoparticles is low. The SEM pictures demonstrate that the nanoparticle size is not uniform and varies between 100 and 500 nm. The delivery curve for particle size confirms the SEM observation, indicating that the nanoparticle dimensions range from 150 to 300 nm, as shown in the figure[22].

#### 4.0.4 Zeta potential

The effect of modifying the surface can be evaluated by examining the surface charge, the density of functional groups, or an enhancement in surface hydrophobicity. To assess any changes in the surface of nanoparticle suspensions in water-based media, the zeta potential is a commonly employed technique. This method measures the electrical potential of the particles and can be influenced by both the composition of the particles and the surrounding medium [23].

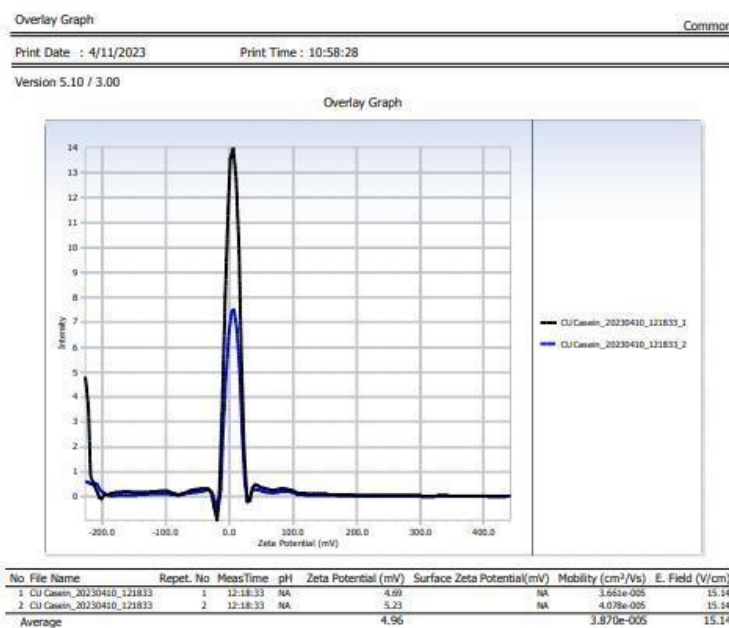


Figure 4 Zeta potential of Cu loaded casein nanoparticles

The primary purpose of measuring the zeta potential is to evaluate the stability of colloidal systems. Particle interactions are critical in determining colloidal stability. The zeta potential plays a crucial role in controlling the repulsive forces among nanoparticles, particularly in aqueous colloidal systems. Electrostatic repulsion acts as the primary stabilizing force in such systems. When the repulsive forces between particles are stronger, it indicates a lower likelihood of aggregation. Nanoparticles in a solution are considered stable if their zeta potential is above ( $\pm$ ) 30 mV, as the surface charge prevents particle aggregation. For this study, the zeta potential of both casein nanoparticles and copper-loaded casein nanoparticles was measured using a Zeta sizer instrument[24]. The distribution of zeta potential was plotted by correlating the zeta potential (in mV) with the intensity (in kcps). The measurements were taken at a count rate of 2,273.3 kcps and a temperature of 25°C. The findings revealed that the zeta potential of CNPs was 39.04 mV. Nevertheless, upon the addition of Cu oxide to the casein nanoparticles, a reduction in the positive potential was noted. More specifically, the zeta potential value of the Cu-loaded casein nanoparticles was measured to be 31.06 mV, as illustrated in Figure 4. The decline in zeta potential can be attributed to the interaction between the positively charged casein macromolecules and the negatively charged oxygen atoms within the Cu oxide. This interaction leads to a reduction in the overall positive charge of the nanoparticles. This interaction causes electrostatic attraction between the particles, which leads to a reduction in the zeta potential[25].

#### 4.0.5 Raman spectral analysis

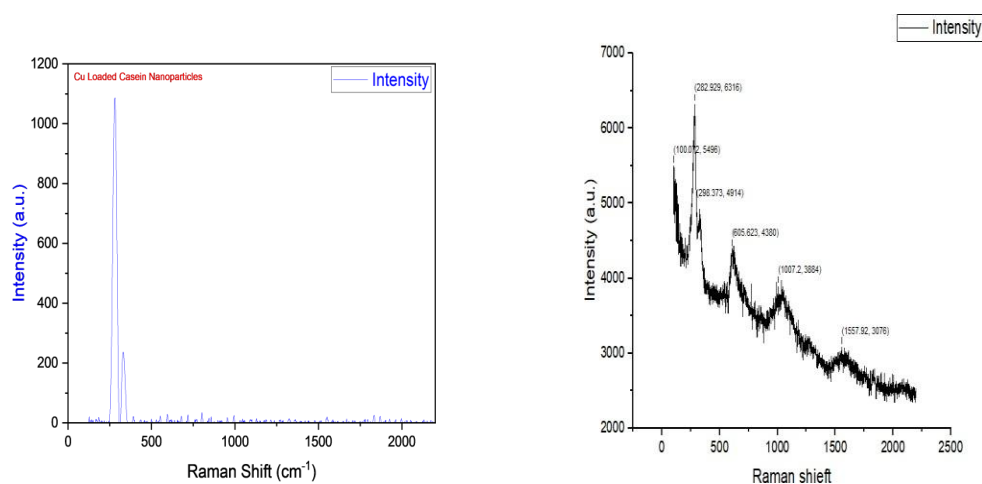


Figure 5 Raman shift of Cu loaded casein nanoparticles

In Figure 5, three Raman active modes were detected at 282 (1/cm), 298 (1/cm), and 605 (1/cm). The Ag mode was identified at 282 (1/cm), while the Bg mode was observed at 298 (1/cm) and 605 (1/cm). The Raman spectra indicate that the sample is made up of a single phase Cu O with a monoclinic structure. As compared to the bulk crystal, the corresponding bands were found to have a red-shift in our samples, which can be attributed to the alteration in the morphology of Cu O. The reported values for the corresponding bands in bulk crystal are 295 (1/cm), 345 (1/cm), and 635 (1/cm)[26].

#### 4.0.6 XPS Analysis

The X-ray photoelectron spectroscopy technique was employed to examine the elemental composition of the samples. Data collection was performed with an energy resolution of 4 eV, and the photoelectron spectrum was recorded for elements such as C 1s, N 1s, O 1s, and Cu 2p. A fine-scan photoelectron spectrum was obtained at a data gaining rate of 0.3 eV and an energy determination of 0.8 eV[27].



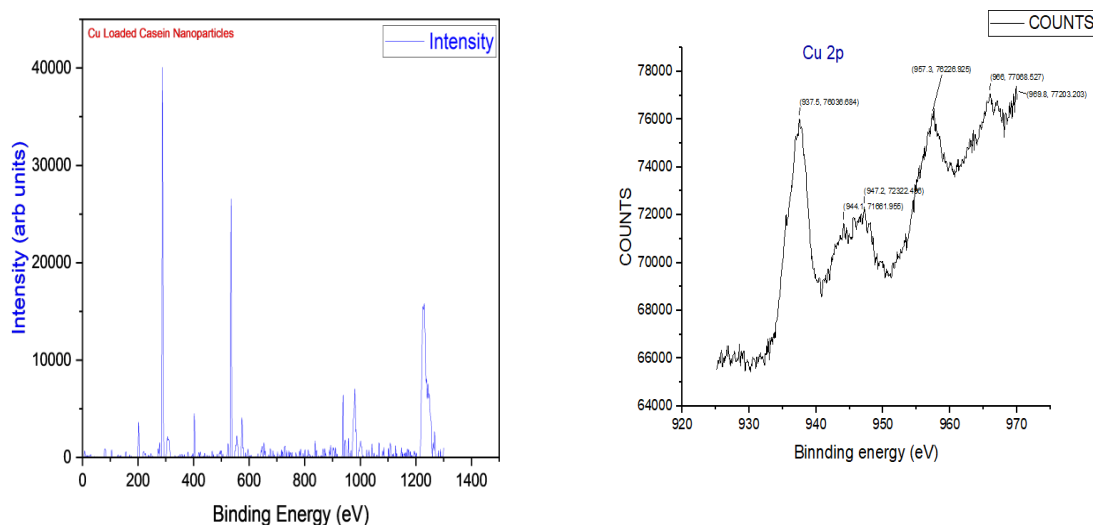


Figure 6 XPS analysis of Cu loaded casein nanoparticles

The Camera Mac3 analyzer was used to analyze the samples using X-ray photoelectron spectroscopy. The data collected had an energy resolution of 4 eV and included fine-scan photoelectron spectrum of C 1s, N 1s, O 1s, and Cu 2p. The analysis revealed that the Cu2p and O1s spectral properties suggested that the formation of CuO lattice particles had occurred (Cu2p<sub>3/2</sub> binding energy - 937.4 eV and O1s binding energy -534.4 eV). Additionally, it was noted that there was an excess of oxygen in the inter-unit space at the contact sites of the nanoparticles, identifiable by a position with a binding energy of 532.2 eV. The low-temperature plasma oxidation process was found to produce a nanostructure, leading to lower thermal stability for the copper oxide formed as compared to crystalline oxide Cu<sub>2</sub>O[28].

### 5.0 Release kinetics of Cu:

The quantity of Fe released from casein nano-particles was evaluated using UV spectroscopy to determine the absorbance at 450 nm. Cu oxide loaded casein nano-carriers displayed slow and sustained release behaviour in water for 3 hours. The encapsulation efficiency of Cu<sub>2</sub>O loaded casein Nano-carriers was measured spectrophotometric in samples containing 0.1 g of Cu-loaded casein Nano-carriers in 10 ml water, and the findings are presented in Table 1. The data indicates that the samples have an encapsulation efficiency of over 90%. This high level of encapsulation is likely due to the presence of pores and the hydrophilic properties of the casein nano-carriers. Similarly, a high doping of copper oxide was also achieved[29].

Table 1Release potential of Cu loaded casein Nano-particles Release potential of Cu loaded casein nanoparticles:

Table 1Release potential of cu oxide loaded casein nanoparticles

S.no	Time (min)	Concentration
1	30	.0031
2	60	.0037
3	90	.0044
4	120	.0049
5	150	.0055
6	180	.0061

### 6.0 Zero-order model:

The most desirable method of delivering nano-nutrients would be to follow "zero order kinetics," which means that the release speed remains constant throughout the delivery time. The constant release of Nano-nutrients from a matrix containing insoluble nano-nutrients and different delivery devices is referred to as zero-order release kinetics[30]. The simplest representation of zero-order release is:

$$Qt = Q_0 + K_0 t$$

The curve obtained in the study showed a straight line that indicates zero-order kinetics. The linear regression analysis resulted in a straight line equation with an  $R^2$  value of 0.99357 and a slope of 0.11923, which represents the zero-order rate constant. Nutrient delivery systems that exhibit zero-order release can increase efficiency while reducing toxicity and dosing frequency[31].

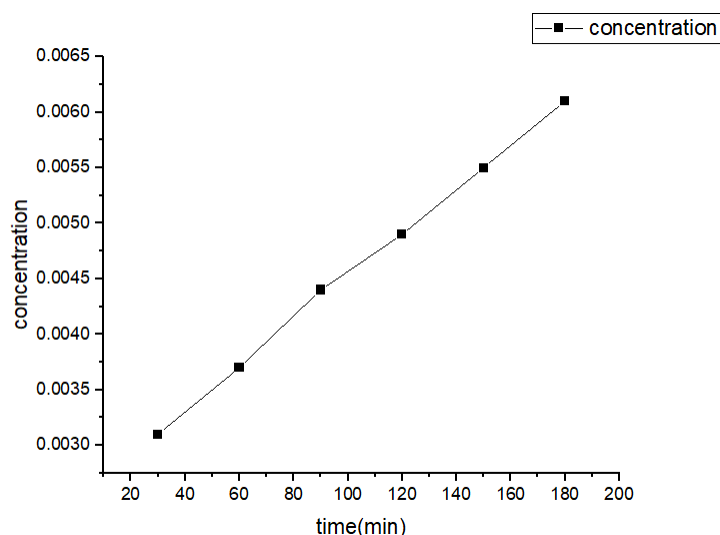


Figure 7Release potential of CuO

### 7.0 Conclusions

In the current study, an emulsion cross-linking technique was used to synthesize casein nanoparticles. The prepared nanoparticles were characterized using a variety of methods, including FTIR and XRD. The cross-linking of casein with glutaraldehyde is confirmed by peaks about 1,683 and 540  $\text{cm}^{-1}$ , indicating that the new substance is biocompatible. Fertilizer is applied to farmland to enhance nutrients for spinach plant development and environmental quality. Chemical fertilizers have a high concentration of soluble nutrients, which plants can absorb right away. Chemical fertilizers, however, may impede soil biological processes, such as accelerating the decomposition of soil organic matter, causing the condition of the soil to degrade. Therefore, biopolymer Nano-carriers are essential in agriculture. According to the study, copper-loaded casein nanoparticles can increase crop yield, nutritional value, and quality while also enhancing soil micronutrient availability through the crop's effective mobilization and translocation of the nutrients to the grains.

## References

1. M. Valcárcel, B.M. Simonet, S. Cárdenas, Analytical nanoscience and nanotechnology today and tomorrow, *Anal. Bioanal. Chem.* 391 (2008) 1881–1887.
2. W.H. Hunt Jr, Nanomaterials: Nomenclature, novelty, and necessity, *Jom.* 56 (2004) 13–18.
3. G. Oberdorster, A. Maynard, K. Donaldson, V. Castranova, J. Fitzpatrick, K. Ausman, J. Carter, B. Karn, W. Kreyling, D. Lai, Group, ArftIRFRSINTSW (2005) Principles for characterizing the potential human health effects from exposure to nanomaterials: elements of a screening strategy, *Part Fibre Toxicol.* 2 (n.d.) 8.
4. C. Buzea, I.I. Pacheco, K. Robbie, Nanomaterials and nanoparticles: sources and toxicity, *Biointerphases.* 2 (2007) MR17–MR71.
5. C.Y. Tai, C.-T. Tai, M.-H. Chang, H.-S. Liu, Synthesis of magnesium hydroxide and oxide nanoparticles using a spinning disk reactor, *Ind. Eng. Chem. Res.* 46 (2007) 5536–5541.
6. T.C.E. Mosha, H.S. Laswai, I. Tetens, Nutritional composition and micronutrient status of home made and commercial weaning foods consumed in Tanzania, *Plant Foods Hum. Nutr.* 55 (2000) 185–205.
7. N. Talreja, D. Chauhan, C.A. Rodríguez, A.C. Mera, M. Ashfaq, Nanocarriers: an emerging tool for micronutrient delivery in plants, *Plant Micronutr. Defic. Toxic. Manag.* (2020) 373–387.
8. M.S. Latha, A. V Lal, T. V Kumary, R. Sreekumar, A. Jayakrishnan, Progesterone release from glutaraldehyde cross-linked casein microspheres: in vitro studies and in vivo response in rabbits, *Contraception.* 61 (2000) 329–334.
9. C.I.C. Crucho, M.T. Barros, Polymeric nanoparticles: A study on the preparation variables and characterization methods, *Mater. Sci. Eng. C.* 80 (2017) 771–784.
10. S. Fu, Z. Sun, P. Huang, Y. Li, N. Hu, Some basic aspects of polymer nanocomposites: A critical review, *Nano Mater. Sci.* 1 (2019) 2–30.
11. A. Roy, S.K. Singh, J. Bajpai, A.K. Bajpai, Controlled pesticide release from biodegradable polymers, *Cent. Eur. J. Chem.* 12 (2014) 453–469.
12. Y. Chen, J. Shi, G. Tian, S. Zheng, Q. Lin, Fe deficiency induces Cu uptake and accumulation in *Commelina communis*, *Plant Sci.* 166 (2004) 1371–1377.
13. M.R. Hussain, R.R. Devi, T.K. Maji, Controlled release of urea from chitosan microspheres prepared by emulsification and cross-linking method, *Iran. Polym. J.* 21 (2012) 473–479.
14. A. Singh, J. Bajpai, A.K. Bajpai, Investigation of magnetically controlled water intake behavior of iron oxide impregnated superparamagnetic casein nanoparticles (IOICNPs), *J. Nanobiotechnology.* 12 (2014) 1–13.
15. A.O. Elzoghby, B.Z. Vranic, W.M. Samy, N.A. Elgindy, Swellable floating tablet based on spray-dried casein nanoparticles: near-infrared spectral characterization and floating matrix evaluation,

- Int. J. Pharm. 491 (2015) 113–122.
16. T. Woggum, P. Sirivongpaisal, T. Wittaya, Properties and characteristics of dual-modified rice starch based biodegradable films, *Int. J. Biol. Macromol.* 67 (2014) 490–502. <https://doi.org/10.1016/j.ijbiomac.2014.03.029>.
  17. B.Z. Butt, I. Naseer, Nanofertilizers, *Nanoagronomy.* (2020) 125–152.
  18. F.-S. Ke, L. Huang, G.-Z. Wei, L.-J. Xue, J.-T. Li, B. Zhang, S.-R. Chen, X.-Y. Fan, S.-G. Sun, One-step fabrication of CuO nanoribbons array electrode and its excellent lithium storage performance, *Electrochim. Acta.* 54 (2009) 5825–5829.
  19. A.S. Abouhaswa, T.A. Taha, Tailoring the optical and dielectric properties of PVC/CuO nanocomposites, *Polym. Bull.* 77 (2020) 6005–6016.
  20. V. Usha, S. Kalyanaraman, R. Thangavel, R. Vettumperumal, Effect of catalysts on the
  21. synthesis of CuO nanoparticles: structural and optical properties by sol–gel method, *Superlattices Microstruct.* 86 (2015) 203–210.
  22. K.K. Dey, P. Kumar, R.R. Yadav, A. Dhar, A.K. Srivastava, CuO nanoellipsoids for superior physicochemical response of biodegradable PVA, *RSC Adv.* 4 (2014) 10123–10132.
  23. M. Elango, M. Deepa, R. Subramanian, A. Mohamed Musthafa, Synthesis, characterization, and antibacterial activity of polyindole/Ag–CuO nanocomposites by reflux condensation method, *Polym. Plast. Technol. Eng.* 57 (2018) 1440–1451.
  24. M.I. Nabila, K. Kannabiran, Biosynthesis, characterization and antibacterial activity of copper oxide nanoparticles (CuO NPs) from actinomycetes, *Biocatal. Agric. Biotechnol.* 15 (2018) 56–62.
  25. L. Miao, C. Wang, J. Hou, P. Wang, Y. Ao, Y. Li, B. Lv, Y. Yang, G. You, Y. Xu, Enhanced stability and dissolution of CuO nanoparticles by extracellular polymeric substances in aqueous environment, *J. Nanoparticle Res.* 17 (2015) 1–12.
  26. M. Verma, V. Kumar, A. Katoch, Sputtering based synthesis of CuO nanoparticles and their structural, thermal and optical studies, *Mater. Sci. Semicond. Process.* 76 (2018) 55–60.
  27. A.I. Stadnichenko, A.M. Sorokin, A.I. Boronin, XPS, UPS, and STM studies of nanostructured CuO films, *J. Struct. Chem.* 49 (2008) 341–347.
  28. T. Ghodselahi, M.A. Vesaghi, A. Shafiekhani, A. Baghizadeh, M. Lameii, XPS study of the Cu@Cu<sub>2</sub>O core-shell nanoparticles, *Appl. Surf. Sci.* 255 (2008) 2730–2734.
  29. H. Naatz, B.B. Manshian, C. Rios Luci, V. Tsikourkitoudi, Y. Deligiannakis, J. Birkenstock, S. Pokhrel, L. Mädler, S.J. Soenen, Model-based nanoengineered pharmacokinetics of iron-doped copper oxide for nanomedical applications, *Angew. Chemie.* 132 (2020) 1844–1852.
  30. S. Weitz, O. Perlman, H. Azhari, S.S. Sivan, In vitro evaluation of copper release from MRI-visible, PLGA-based nanospheres, *J. Mater. Sci.* 56 (2021) 718–730.
  31. Y. Yechekel, I. Dror, B. Berkowitz, Catalytic degradation of brominated flame retardants by copper oxide nanoparticles, *Chemosphere.* 93 (2013) 172–177.